sustainability

MDPI

Article

Novel Synthesis of Carbon Dots from Coconut Wastes and Its Potential as Water Disinfectant

Subramani Krishnaraj Rajkishore [1,*], Krishnagounder Padmanaban Devadharshini [1], Ponnuraj Sathya Moorthy [2], Vanniya Sreeramulu Reddy Kiran Kalyan [3], Rajkishore Sunitha [1], Mohan Prasanthrajan [2], Muthunalliappan Maheswari [1], Kizhaeral Sevathapandian Subramanian [2], Nalliappan Sakthivel [4] and Ruben Sakrabani [5]

[1] Department of Environmental Sciences, Tamil Nadu Agricultural University, Coimbatore 641003, India
[2] Centre for Agricultural Nanotechnology, Tamil Nadu Agricultural University, Coimbatore 641003, India
[3] Department of Soil Science and Agricultural Chemistry, Tamil Nadu Agricultural University, Coimbatore 641003, India
[4] Agricultural Research Station, Tamil Nadu Agricultural University, Bhavanisagar 638451, India
[5] Cranfield Soil and Agrifood Institute, School of Water, Energy & Environment, Cranfield University, Cranfield MK43 0AL, UK
* Correspondence: rajkishoresk@gmail.com; Tel.: +91-9500212743

Abstract: This paper presents a facile and effective method for the large-scale production of carbon dots (CDs) from diverse coconut wastes (fronds, husk and shell). On comparing two different methods, namely (i) hydrothermal carbonization and (ii) novel sequential synthesis processes (pyrolysis followed by sonication), the latter procedure recorded a higher recovery of CDs (14.0%) over the hydrothermal method (2.33%). Doping agents such as urea, polyethyleneimine (PEI) and hexamethylenetetramine (HMTA) were chosen at varying concentrations to synthesize surface-modified CDs (SMCDs) for enhanced antibacterial properties. Among these SMCDs, urea-doped CDs $_{(1:1)}$ @ 1000 ppm registered significantly higher cytotoxicity (20.6%) against *Escherichia coli* (*E. coli*). Subsequently, to assess the applicability of CDs as a disinfectant in water purification systems, two products, namely (i) CD-infused chitosan beads and (ii) pelletized CDs, were developed to ensure the immobilization of CDs. Studies with lab-scale prototypes have revealed that CDs infused chitosan beads reduced the colonies of *E. coli* from 5.41×10^2 CFU/mL (control group) to 2.16×10^2 CFU/mL, in comparison with pelletized CDs that decreased to 3.30×10^2 CFU/mL. The biosafety of CDs was assessed against *Eisenia fetida* for 21 days, and the observations revealed no mortality, even at 2000 ppm. Overall, this research demonstrated that a waste biomass can be effectively transformed into a novel water disinfectant. Furthermore, this scientific endeavor opens up research avenues to evolve advanced water purifiers using low-cost and eco-friendly nanomaterials.

Keywords: coconut waste; carbon dots; cytotoxicity; *Escherichia coli*; *Eisenia fetida*; water disinfectant

Citation: Rajkishore, S.K.; Devadharshini, K.P.; Sathya Moorthy, P.; Reddy Kiran Kalyan, V.S.; Sunitha, R.; Prasanthrajan, M.; Maheswari, M.; Subramanian, K.S.; Sakthivel, N.; Sakrabani, R. Novel Synthesis of Carbon Dots from Coconut Wastes and Its Potential as Water Disinfectant. *Sustainability* **2023**, *15*, 10924. https://doi.org/10.3390/su151410924

Academic Editors: Jesús G. Ovejero and Alvaro Gallo Cordova

Received: 25 May 2023
Revised: 5 July 2023
Accepted: 8 July 2023
Published: 12 July 2023

1. Introduction

Carbon dots (CDs) are new-generation carbon nanomaterials with a characteristic diameter size less than 10 nm that were serendipitously discovered in 2004 at the time of purification of single-wall carbon nanotubes (SWCNTs) [1]. In recent days, CDs have gained a lot of attention among researchers because of their smallest size, tunable characteristics, low toxicity, biocompatibility and cheaply available precursors for synthesis [2]. With these intriguing characteristics, CDs have now emerged as a promising substitute for metal-based quantum dots, with applications in bioimaging and photocatalysis [3], while simultaneously opening up research avenues to resolve several environmental issues with their unique surface chemistry [4].

The contamination of drinking water is one of the major health concerns that are witnessed worldwide. Globally, 3 out of 10 people, or 2.1 billion people, lack access to

safe and readily available water at home, and 6 out of 10 people, or 4.5 billion people, lack access to safely managed water (WHO and UNICEF 2017). Every year, waterborne infections claim millions of lives globally, with the majority of these deaths occurring in developing nations [5]. Hence, the development of cost-effective and environment-friendly water disinfection technologies is the need of the hour. At this juncture, CDs, which have been reported to have antibacterial activity [6,7] while demonstrating nontoxicity in mammalian systems and with a large opportunity of being synthesized from diverse waste biomasses [8], makes this as a good candidate for exploring their potential as a water disinfection agent.

Among the various agricultural wastes, the coconut waste biomass is considered a sustainable, cheap and alternative feedstock for the preparation of carbon dots [8–10]. Despite the fact that coconut wastes such as shells and husks have been reported as precursors for the synthesis of CDs, none of the published protocols favor large-scale production; in addition, a systematic study is still lacking to demonstrate CDs' ability as a water disinfection agent. Several review papers [11,12] have been published to highlight the scope and prospectus of applying CDs in various environmental applications as organic pollutant reduction through photocatalysis, pollutant ion sensing and heavy metal detection, as well as reduction, adsorption treatment and membrane fabrication. Despite the fact that CDs are considered as potent new age antimicrobial agents, numerous works have only elucidated the potential of varied properties of CDs as a bactericidal effect and documented possible mechanisms of action [13], while very limited papers have been reported to illustrate the employability of biomass-derived pristine/bare CDs as water disinfectants in purification systems. Nevertheless, the ability of CDs as nanocomposites, such as multiple-core@ shells [14], CD-loaded $Co_xNi_{1-x}Fe_2O_4$ and x = 0.9/SiO_2/TiO_2 [15] for water disinfection by enhancing the photocatalytic performance has been reported [16]. However, the potential of biomass-derived pristine CDs and/or surface-modified CDs for disinfection in a water medium through light independent reactions has rarely been studied. Hence, this research was proposed to address two challenges, namely the lower yield of CDs and unexplored immobilization platforms for CDs, that hinder the wide application of CDs in general and as a water disinfectant in particular.

With this background, it was hypothesized that CDs with their unique surface chemistry owing to their high surface area-to-mass ratio and associated tunable properties can exhibit antimicrobial activity against waterborne pathogens, paving the way for the development of sustainable technology from waste biomasses. Hence, this study was undertaken to demonstrate the potential of coconut wastes for transformation into CDs with water disinfection properties. Moreover, this research also focused on evolving a suitable synthesis method that favors the large-scale production of CDs from waste biomasses so as to ensure sustainable solutions. Hydrothermal synthesis has been considered to be a simple, inexpensive and eco-friendly method to synthesize CDs [17,18]. However, the percent of recovery of CDs through this protocol is very low [10]. Thus, two novel sequential processes (pyrolysis, followed by sonication) were evolved to assess the potential to obtain the maximum recovery of CDs. Furthermore, surface = modified CDs with dopants (urea, PEI and HMTA) were also synthesized to improve their antimicrobial properties [19–21]. In this study, to assess the potential of synthesized CDs as a water disinfection agent, CDs were tested against *Escherichia coli*, a common indicator of fecal matter contamination in drinking water. Subsequently, the compatibility of CDs with a suitable matrix (chitosan beads) was also explored to ensure the effective immobilization of CDs without losing their inherent propensity for application in water disinfection systems.

2. Materials and Methods

Coconut wastes (fronds, husks and shells) were collected from the coconut residue processing unit located at Pollachi in Tamil Nadu, India. The coconut wastes were washed, air-dried and ground to a fine powder using an impact pulverizer and sieved under a British

Standard Sieve (BSS) 200 (75-micron mesh) to obtain uniform-sized particles and stored in airtight plastic containers until use. Distilled water was used throughout the experiments.

2.1. Synthesis of Carbon Dots

2.1.1. Hydrothermal Carbonization

Carbon dots were synthesized by the hydrothermal carbonization method by employing a hydrothermal reactor (Model: Trident Labortek; 100 mL, non-stirred autoclave), as optimized by Abinaya et al. [10]. Three grams of the powdered coconut waste was added to 75 mL of distilled water in a ratio of 1:25. Subsequently, the mixture was transferred into a 120 mL hydrothermal reactor and heated at 250 °C for 6 h. Then, the solution was subjected to centrifugation at 10,000× *g* rpm for 20 min to remove the larger particles. Followed that, the solution was filtered using a 0.22 µm syringe filter and then finally dried in a hot air oven for 48 h to obtain the CDs.

2.1.2. Two Sequential Synthesis Processes

Methods such as pyrolysis and sonication have been employed separately to synthesize CDs/carbon nanomaterials [22,23]. However, in this study, to ensure that the synthesized CDs are below the size of 10 nm, though the majority of the particles are within this size regime, two sequential processes, namely pyrolysis (muffle furnace) followed by sonication (probe sonicator), were adopted as a maiden attempt to assess their potential to improve the yield of CDs. Muffle furnace (Model: Sonics) and Probe sonicator (Model: Indfurr, India) were employed. The precursor materials (coconut wastes) were initially subjected to four hours of pyrolysis in a muffle furnace at 700 °C for the shell powder and 250 °C for the fronds and husks. The resultant product was ground to fine powder in a grinder. It was then sieved through a 0.09 mm Indian Standard (IS) sieve.

As the second step, the carbonized powder obtained after pyrolysis (1 g) was sufficiently dissolved in 25 mL of distilled water, and the mixture was then sonicated after optimization for 15 min and 90% amplitude at room temperature. To separate the supernatant liquid from the carbon precipitate, the solution was centrifuged at 10,000× *g* rpm for 10 min. The settled particles were collected and dried in a hot air oven at 80 °C for 12 h. CDs obtained as dried powder were collected and macerated with pestle and mortar and then subjected to further characterization and confirmation.

2.2. Synthesis of Surface-Modified CDs

CDs were characterized as mentioned below (Section 2.3), and it was observed that the synthesized CDs were anionic in nature. Hence, this modified protocol was adopted to promote amine functionalization by adding urea/polyethyleneimine (PEI)/hexamethylenetetramine (HMTA) so as to synthesize N-doped CDs. All the experiments were conducted with sufficient replications (three replications repeated three times), synthesized CDs were rigorously confirmed through various characterization techniques (Section 2.3) and the data were cross-examined with each parameter to ascertain the reproducibility of the protocol to obtain homogeneity of the CDs.

All the surface-modified carbon dots were synthesized from coconut shell powder as a precursor material, since the smallest size CDs (7 nm) was achieved from the coconut shells when compared to the CDs (15 nm) from the fronds and shells (9 nm). The surface charge-modifying agents, namely urea, PEI and HMTA, were purchased from Central Drug House (P) Ltd. (Delhi, India), Sigma Aldrich (St. Louis, MO, USA) and SDFCL (Chennai, India), respectively.

2.2.1. Urea-Doped CDs

Coconut shell powder obtained from muffle furnace was taken and mixed with distilled water in the ratio (biomass:water) of 1:25. To prepare four types (urea-doped CDs $_{(1:1)}$; urea-doped CDs $_{(1:2)}$; urea-doped CDs $_{(1:3)}$; urea-doped CDs $_{(1:4)}$), four different urea concentrations of 1, 2, 3 and 4 g were individually poured into each beaker. It was then

subjected to stirring at 280 rpm for 24 h in magnetic stirrer followed by sonication (90% amplitude for 15 min) and centrifugation (10,000× *g* rpm for 10 min). Finally, the settled particles were dried under hot air oven at 80 °C for 12 h and Urea-doped CDs (four types) were obtained.

2.2.2. PEI-Doped CDs

Coconut shell powder obtained from a muffle furnace was used and mixed with distilled water in a ratio (biomass:water) of 1:25. To prepare three types of PEI-doped CDs, three different PEI concentrations of 0.5, 1.0 and 1.5 g were individually poured into each beaker. Ten milliliters of distilled water was added to each beaker and subjected to magnetic stirring at 280 rpm for 20 min. Different concentrations of PEI that were available in the three beakers were added to the coconut shell powder mixture and subjected to ultrasonication for 15 min at 90% amplitude. The resultant solution was centrifuged at 10,000× *g* rpm for 10 min. The settled particles (PEI-doped CDs $_{(0.5:1)}$, PEI-doped CDs $_{(1:1)}$ and PEI-doped CDs $_{(1.5:1)}$) were collected and dried at 80 °C in a hot air oven for 12 h.

2.2.3. HMTA-Doped CDs

Coconut shell powder obtained from a muffle furnace was mixed with distilled water in a ratio (biomass:water) of 1:10. Then, 1 g of HMTA was added to this coconut shell powder mixture. It was then subjected to stirring at 280 rpm for 10 min with a magnetic stirrer, followed by sonication (90% amplitude for 15 min) and centrifugation (10,000× *g* rpm for 10 min). Finally, the settled particles were dried in a hot air oven at 80 °C for 12 h, and HMTA-doped CDs $_{(1:1)}$ were obtained.

2.3. Characterization of CDs

The size and morphology of the synthesized CDs were analyzed using high-resolution transmission electron microscopy (JEOL, Tokyo, Japan) and scanning electron microscope (SEM) (FEI, Quanta 250, Hillsboro, OR, USA), respectively. The average particle size was measured with a Gaussian fitting curve using ImageJ software (version: 1.8.0). The crystal structure of the material was determined by selected area electron diffraction (SAED) of a high-resolution transmission electron microscope (HR-TEM), and it was verified using an X-ray diffractometer (Shimadzu Model, Make XRD 600, Rigaku, Japan). The optical properties were determined with a UV–Vis spectrophotometer (Specord 210 plus, Jena, Germany) in the range 190–1100 nm. The functional groups, as well as chemical bonding, of the CDs were recorded by employing Fourier-transform infrared (FTIR) (Jasco Model: R-3000-QE, Woburn, MA, USA). The data obtained were plotted using ORIGIN Ver.8.5. The zeta potential was measured using a nanoparticle size analyzer (HORIBA-SZ-100, Kyoto, Japan), in which the zeta potential was measured between −200 mV and +200 mV. The pH of the solution was adjusted to neutral before measuring the zeta potential, as outlined by Qiang et al. [24].

2.4. Assessment of Antimicrobial Activity of CDs

Escherichia coli, an indicator of fecal matter contamination in drinking water, was used as the test species to assess the potential of the synthesized CDs as a water disinfection agent.

Lactate Dehydrogenase (LDH) Assay

The effect of CDs on the integrity of *E. coli* cell membranes was assessed using the LDH assay (Kit: EZCount, CCK036, Thane, India). The study comprised nine treatments, namely pristine CDs, PEI $_{(0.5:1)}$-doped CDs, PEI $_{(1:1)}$-doped CDs, PEI $_{(1.5:1)}$-doped CDs, urea-doped CDs $_{(1:1)}$, urea-doped CDs $_{(2:1)}$, urea-doped CDs $_{(3:1)}$, urea-doped CDs $_{(4:1)}$ and HMTA-doped CDs $_{(1:1)}$. Briefly, *E. coli* was cultured in triplicate in Luria Bertani media at 34 °C overnight. Cells cultured were treated with all the treatments at a concentration of 1000 ppm (1 mg/mL, *w*/*v*), which was dispersed in the media by sonication at 40%

amplitude for 4 min. The log phase and stationary phase for the chosen culture were at the 3rd and 9th hours, respectively. Accordingly, at the 3rd and 9th hours of incubation, the culture supernatant was collected by centrifugation and incubated with the LDH reaction mixture in a 96-well plate. For the positive control wells, a lysis solution was added to obtain the maximum LDH release control, and untreated cells were taken as the negative control. All the assay treatments were carried out in 3 replications. The absorbance values were taken at 490 nm and 600 nm using a spectrophotometric multi-well plate reader. LDH was quantified using the following Formula (1):

$$\text{LDH } \% = 100 \times (A - C/B - C) \quad (1)$$

where A = average (Avg) absorbance of the test − Avg absorbance of the background control, B = Avg absorbance of the maximum LDH control − Avg absorbance of the volume correction control and C = Avg absorbance of the untreated control − Avg absorbance of the background control.

2.5. Development of CD-Based Prototypes to Assess the Water Disinfection Potential

2.5.1. Synthesis of CD-Infused Chitosan Beads

To immobilize the CDs, chitosan beads were selected as a platform for infusing the CDs into chitosan beads. CD (urea-doped CDs $_{(1:1)}$)-infused chitosan beads were synthesized as outlined by Yan et al. [25].

2.5.2. Synthesis of CDs Pellets

CDs were made into pellets using a tablet pressing machine (RIMEK, PC 20). To enhance the compactness of the synthesized CD pellets, 4% PVA (polyvinyl amine) was added as a binding agent to the CDs. The resultant CD pellets were air-dried for 2 h with an average weight of 600 mg.

2.6. Assessing the Water Disinfection Potential of CDs

The water disinfection potential of CD-infused chitosan beads and pelletized CDs were assessed with the fabricated lab-scale prototype. Fifty grams each of CD $_{(1:1)}$-infused chitosan beads and CD pellets were loaded into the specific cartridges. For this prototype, 50 mL of sterile water and 50 µL of overnight-grown *E. coli* culture (known load) were added and left for filtration. At every 2 h interval (2, 4 and 6 h), 100 µL of sample was retrieved to analyze the colony-forming units using the spread plate technique, and the initial control culture was found to have >5.41 × 10^2 CFU/mL.

2.7. Biosafety Studies of Synthesized CDs

The acute toxicity study of pristine CDs and urea-doped SMCDs (urea-doped CDs $_{(1:1)}$) at four different concentrations (250, 500, 1000 and 2000 ppm) were assessed against earthworms by adopting the filter paper contact test as per OECD TG (207). Whatman no. 1 filter paper was placed in the petri dish, and 2 mL of CD solution was added to the filter paper. Two adult earthworms in each petri dish were exposed to the above CD concentrations. All experiments were carried out in the dark at 20 °C for 48 h. The observations were recorded continuously for 21 days at 24 h intervals. The mortality % was calculated and recorded. Worms were considered dead when they did not respond to touch of the anterior region. The results of the treatment group were analyzed to estimate the mortality of the earthworms upon exposure to CDs.

2.8. Statistical Analysis

The data obtained from the above experiments were statistically analyzed using Origin software version 8.5.

3. Results and Discussion

This study demonstrated that a higher recovery of CDs (14.7%) from coconut wastes could be possible when these biomasses were subjected to sequential processes (pyrolysis, followed by sonication), while the hydrothermal method showed a minimal recovery percentage of 2.33%. In the hydrothermal carbonization method, the biomass/raw material first undergoes hydrolysis, followed by dehydration, and subsequently, aromatization, decarboxylation, polymerization and aldol condensation reactions take place and lead to the formation of aromatic clusters, and if the aromatic concentration reaches a critical supersaturation point, a burst nucleation takes place, and CDs are ultimately formed [26].

In the sequential processes (pyrolysis, followed by sonication), the first process favors the conversion of biomass into CDs by mechanisms such as drying, followed by the release of volatile substances and the development of a carbon core as a consequence of the conversion of cellulose, hemicellulose and lignin [20]. On the other hand, the sonication method is also well reported for its ability to synthesize CDs [27,28]. During the sonication process, the underlying mechanisms such as the production of a strong hydrodynamic shear force by means of high- or low-pressure waves generate and distribute tiny vacuum bubbles into the liquid, which favors the formation of CDs by splitting the carbon bonds [29]. Overall, the combination of the two methods yielded a higher recovery, and these sequential processes are considered to be highly beneficial for the large-scale production of CDs from waste biomasses.

3.1. Size, Morphology, Crystallinity and Stability of CDs

The HR-TEM images showed that the CDs synthesized from fronds, husks, shells and urea-doped CDs $_{(1:1)}$ were in the range of 15, 9, 7 and 7 nm, respectively (Figures 1a, 2a, 3a and 4a), which is consistent with the results of Baweja and Jeet [30], who synthesized carbon quantum dots (CQD) and two different graphene quantum dots (GQD1 and GQD2) in the size range between 3 and 15 nm that were derived from sugarcane bagasse. It is clear from the images that CDs are spherical in shape and dispersed uniformly. The selected area electron diffraction (SAED) portrayed in Figures 1c, 2c, 3c and 4c showed diffused rings, which indicates the poly-nanocrystalline nature of CDs [31]. The zeta potential of all the synthesized CDs, as given in Table 1, was found to be negative, which indicates that the surfaces of CDs have negative charged moieties like hydroxyl and carboxylate groups [23,32] that aid in achieving a good dispersion in water [22]. The addition of urea during the synthesis process also resulted in the synthesis of anionic CDs. This result is consistent with the results of Arvapalli et al. [33], who synthesized urea-doped carbon dots with citric acid as precursor materials in a ratio of 1:1 and found that the zeta potential was -38.5 ± 2.72 mV. Despite the fact that urea contributes to amine groups, urea-doped CDs in a ratio of 1: 1 did not exhibit positive zeta potential. This may be due to the fact that a higher ratio of COO- groups on the surfaces of CDs/precursors could not be outnumbered by positively charged functional groups of urea.

Table 1. Size, morphology, crystallinity and surface charge of carbon dots derived from coconut waste.

S. No.	Precursor Material	Average Size (nm)	Shape	Zeta Potential (mV)
1.	CDs $_{(Fronds)}$	15	Spherical	−22.4
2.	CDs $_{(Husk)}$	9	Spherical	−28.8
3.	CDs $_{(Shell)}$	7	Spherical	−14.8
4.	Urea-doped CDs $_{(1:1)}$	7	Spherical	−33.3

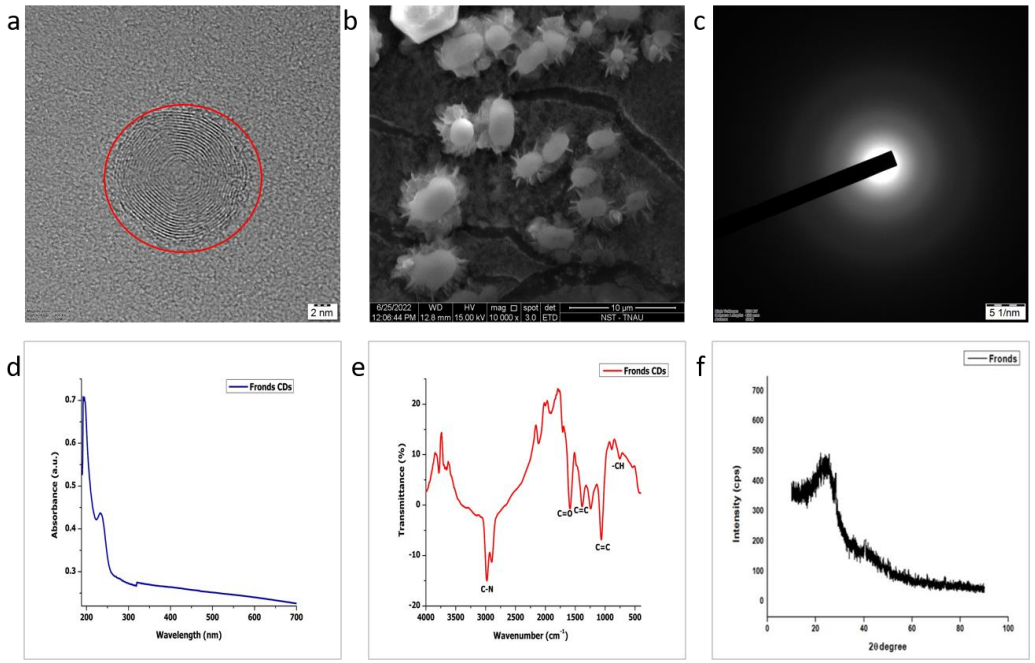

Figure 1. Characterization of CDs derived from coconut fronds. (**a**) HR-TEM (Red circle shows the lattice structure of carbon dot). (**b**) SEM. (**c**) SAED pattern. (**d**) UV-Vis spectrum. (**e**) FTIR peaks. (**f**) XRD pattern.

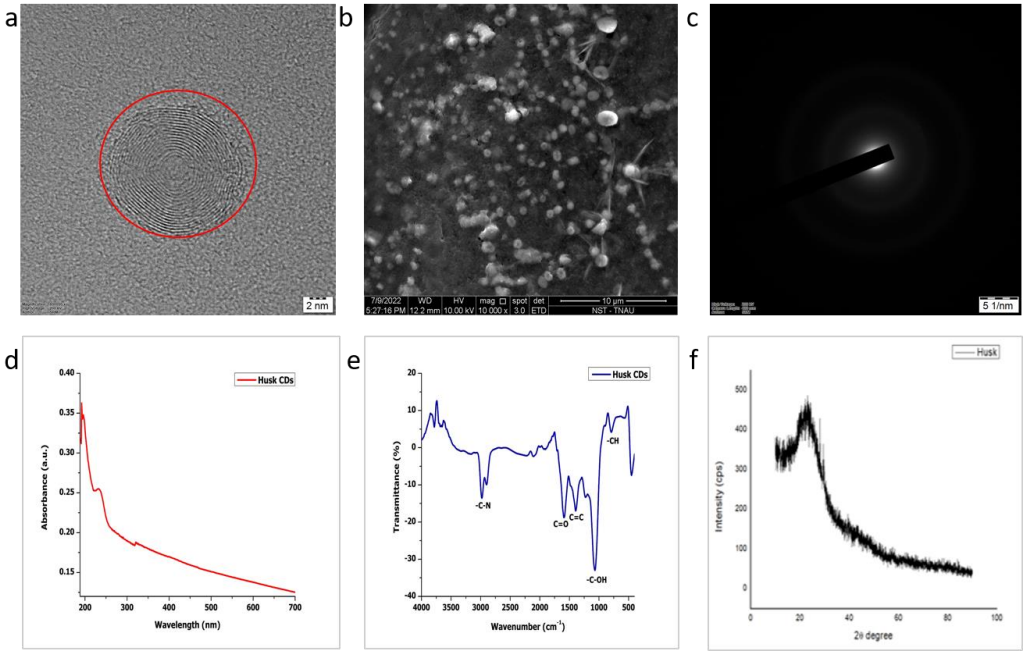

Figure 2. Characterization of CDs derived from coconut husks. (**a**) HR-TEM (Red circle shows the lattice structure of carbon dot). (**b**) SEM. (**c**) SAED pattern. (**d**) UV-Vis spectrum. (**e**) FTIR peaks. (**f**) XRD pattern.

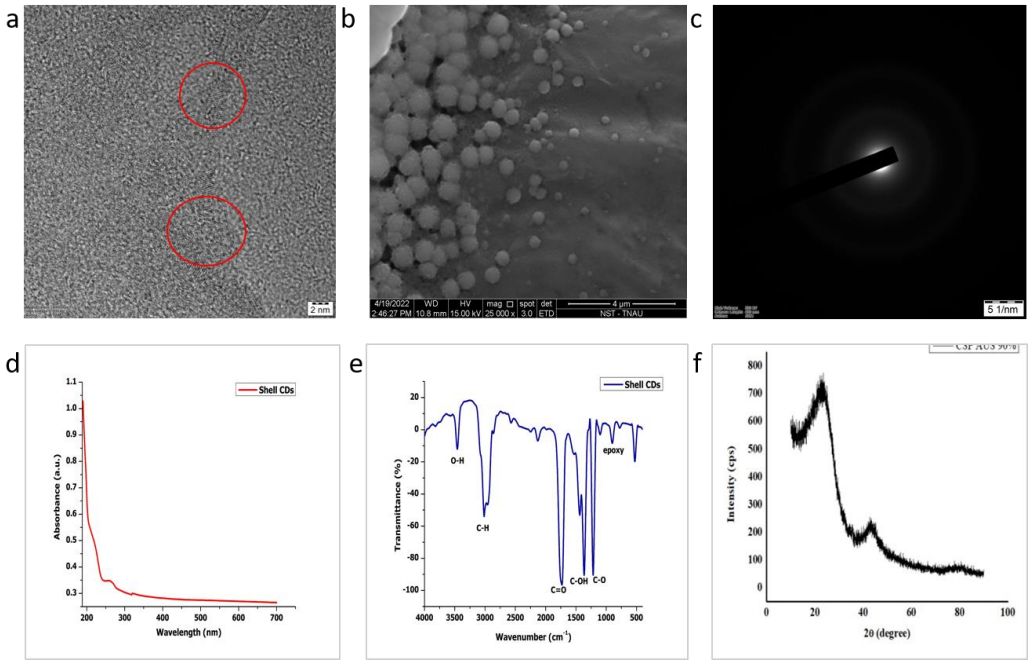

Figure 3. Characterization of CDs derived from coconut shells. (**a**) HR-TEM (Red circle shows the lattice structure of carbon dot). (**b**) SEM. (**c**) SAED pattern. (**d**) UV-Vis spectrum. (**e**) FTIR peaks. (**f**) XRD pattern.

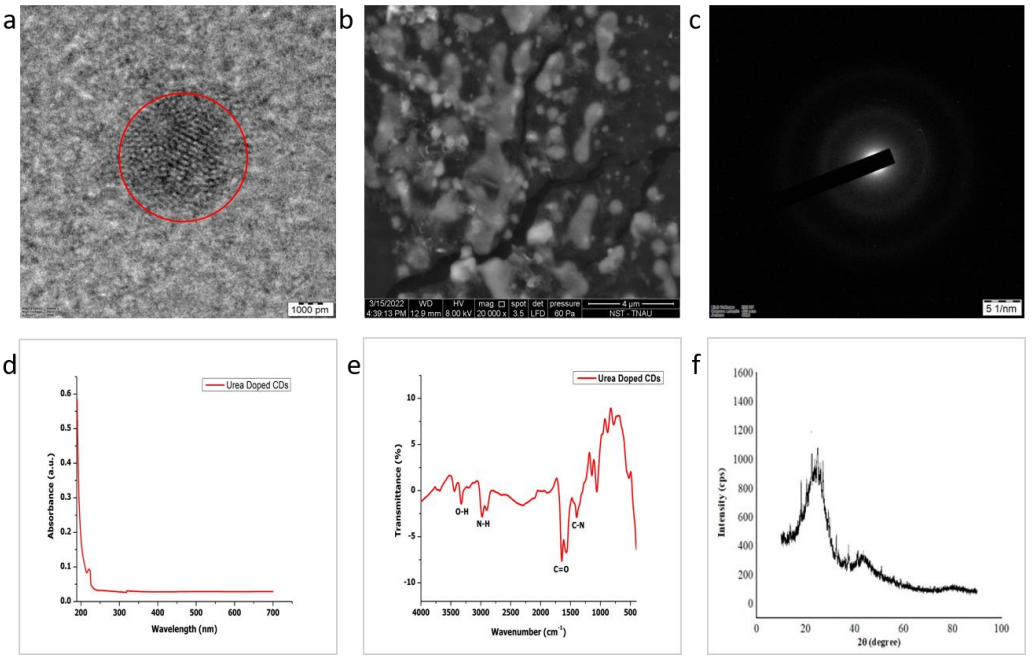

Figure 4. Characterization of urea-doped CDs $_{(1:1)}$. (**a**) HR-TEM (Red circle shows the lattice structure of carbon dot). (**b**) SEM. (**c**) SAED pattern. (**d**) UV–Vis spectrum. (**e**) FTIR peaks. (**f**) XRD pattern.

3.2. Optical Studies

The optical properties of CDs from fronds, husks, shells and urea-doped CDs $_{(1:1)}$ were investigated using the UV–Vis absorption spectrum, and the corresponding results are exhibited in Figures 1d, 2d, 3d and 4d. First, the absorption peak was observed at 226 nm for the CD-derived fronds and husks and at 263 nm for the CDs derived from shells. Secondly, the shoulder peak was observed for all the three types of CDs. These two peaks were mainly raised due to the existence of the π–π* transition and n–π* transition of C=O

bonds. This finding is in line with the results of Dager et al. [22], who synthesized carbon quantum dots from fennel seeds by using the pyrolysis method.

3.3. Fourier-Transform IR Spectroscopy

The FTIR spectroscopic investigations of carbon dots are depicted in Figures 1e, 2e and 3e. The evidence of hydrophilic surfaces on CDs from the shells was confirmed by the formation of the O-H stretching vibration, as denoted by the intense peak at 3440 cm^{-1} [34]. The peaks at 3022 and 2970 cm^{-1} were attributed to the C-H stretching vibration. Furthermore, it also displayed the stretching bands of C=O at 1738 cm^{-1}, which is a specific feature of CDs [32], -OH bending at 1442 cm^{-1}, C-OH at 1375 cm^{-1}, C–O stretching at 1213 cm^{-1} and epoxy at 918 cm^{-1}. These results coincide with the FTIR spectrum dataset of Manoharan et al. [35], who synthesized fluorescent carbon dots from tender coconut water using the acid-assisted ultrasonic route, whereas, in the cases of the fronds and husks, the major peak obtained at 2974 cm^{-1} corresponded to the C-N and C-H stretching vibrations. The C=C stretching vibration was observed at 1378 cm^{-1} [36], and the peaks at 1230, 1051 and 805 corresponded to the C-O-C, -C-OH and -CH bands [37], respectively.

Surface-modified carbon dots with urea as the doping agent showed a peak at 3323 cm^{-1} (Figure 4e). Arvapalli et al. [38], who synthesized urea-modified carbon dots from citric acid and urea in a ratio of 1:1, showed that the peak range between 3000 and 3500 cm^{-1} with the stretching vibrations of O-H and N-H corresponded to the carboxylic acid and amine groups, respectively. The characteristic O-H bending was observed at the peak value of 1655 cm^{-1} [38]. Simultaneously, the peak at 1574 cm^{-1} was associated with the C-N stretching vibration, indicating the formation of -CONR [39].

3.4. X-ray Diffraction (XRD)

The XRD patterns of CDs derived from fronds, husks and shells, as well as urea-modified CDs $_{(1:1)}$ (Figures 1f, 2f, 3f and 4f), evidently displayed the fingerprints of CDs with two peaks, namely a broad peak ($2\theta = 23.4^{o}$) that confirmed CDs have disordered carbon [35,40] and a weak shoulder peak ($2\theta = 42.5^{o}$) that could have favorably occurred due to the graphitic carbon core in CDs. From this observation, it can be presumed that the structures of the CDs obtained from all the three coconut wastes and surface-modified CDs have two sections, an amorphous layer and a minor portion of a crystalline layer. These findings are in line with the observations of Manoharan et al. [35] and Zheng et al. [41].

3.5. EDAX (Energy-Dispersive Analysis of X-ray)

The EDAX (Table 2 and Figure 5) showed that the synthesized carbon dots contain the highest weight percentage of carbon, followed by oxygen, which indicates that the carbon dots are highly pure in nature [36].

Table 2. Elemental compositions of the carbon dots.

Elemental Composition	CDs (Fronds)	CDs (Husk)	CDs (Shell)	Urea-Doped CDs
Carbon	90.41	91.46	95.82	94.74
Oxygen	9.59	8.54	2.57	3.26

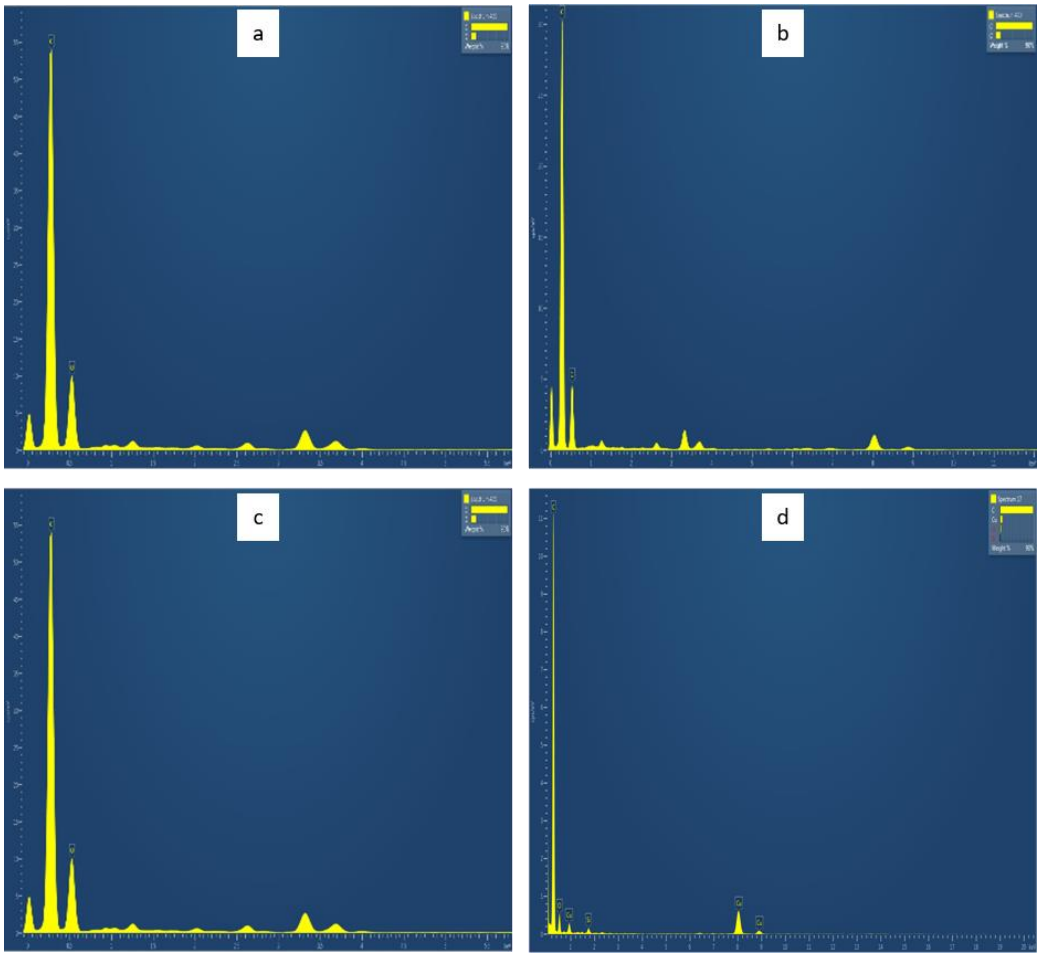

Figure 5. EDAX graph showing the elemental compositions of CDs derived from (**a**) fronds, (**b**) husks, (**c**) shells and (**d**) urea-doped CDs $_{(1:1)}$.

3.6. Surface Area and Pore Size

The total surface area of the carbon dots was obtained by using both the Langmuir method and multi-point Brunauer–Emmett–Teller (BET) method. The increased surface areas of CDs when compared to their respective precursor materials confirmed the size reduction [42,43]. The corresponding summary of the surface area, total pore volume and average pore diameter is tabulated in Table 3.

Table 3. Surface area characteristics of pristine CDs and SMCDs.

CDs	Average Pore Radius (nm)	Total Pore Volume (cc/g)	BET Method (m^2 g^{-1})	Langmuir Method (m^2 g^{-1})
CDs $_{(Fronds)}$	4.31	0.03	12.9	361
CDs $_{(Husk)}$	2.09	0.02	18.0	1478
CDs $_{(Shell)}$	1.97	0.02	139	4535
Urea-doped CDs $_{(1:1)}$	1.73	0.01	99.1	3653

3.7. Antibacterial Activity of Synthesized CDs

The LDH study was employed for assessing the antibacterial activity of CDs. At the end of the third hour of the growth phase of *E. coli*, which was the early exponential stage, the results showed that the % cytotoxicity at the concentration of 1000 ppm was the maximum for urea-doped CDs $_{(1:1)}$. The CDs without any surface modification showed 4.89% toxicity. On the other hand, CDs modified with PEI did not show any cytotoxicity against *E. coli*, which can be compared with the findings of Devkota et al. [44], who

synthesized amine-functionalized carbon dots with PEI and found no antimicrobial effect on bacterial species like *Agrobacterium*, *Salmonella*, *Pectobacterium* and *E. coli*. Hence, our study showed that doping with urea during CD synthesis contributed to favorable surface modifications in CDs and exhibited antibacterial properties when compared to other doping agents such as PEI and HMTA (Table 4).

Table 4. Comparison of the % cytotoxicity of CDs at the concentration of 1000 ppm against *E. coli* after 3 h of growth.

Treatments	% Cytotoxicity
Pristine CDs	4.89 (±0.24) ^{f}
PEI-doped CDs $_{(0.5:1)}$	1.96 (±0.18) ^{g}
PEI-doped CDs $_{(1:1)}$	1.02 (±0.03) ^{h}
PEI-doped CDs $_{(1.5:1)}$	1.28 (±0.03) ^{h}
Urea-doped CDs $_{(1:1)}$	20.6 (±0.70) ^{a}
Urea-doped CDs $_{(2:1)}$	8.41 (±0.17) ^{c}
Urea-doped CDs $_{(3:1)}$	6.81 (±0.09) ^{d}
Urea-doped CDs $_{(4:1)}$	6.17 (±0.08) ^{e}
HMTA doped CDs	14.6 (±0.35) ^{b}

Data in the parentheses indicate the standard deviation from the mean. Different letters in superscript indicate the existence of significant differences among the treatments.

The antibacterial activity of CDs is a result of a single mechanism of action, or there may be a coexistence of multiple mechanisms, such as (1) physical/mechanical damage to the cell membrane, (2) inhibiting bacterial cell wall synthetases, (3) triggering the cellular production of reactive oxygen species (ROS), (4) disrupting cell membrane electron transport, (5) internalization into the cell, damaging DNA and protein synthesis, (6) affecting the synthesis of bacterial biofilm, etc. [45]. Nevertheless, the most-reported principal mechanism that is responsible for causing toxicity in any biological system by the majority of nanomaterials is its role in creating oxidative stress as a consequence of the excessive production of ROS, and only the reaction pathway to generate ROS varies from one nanomaterial to another [46]. Specific studies undertaken with CDs have also reported that the surface charge plays a key role in causing antibacterial activity [47]. They have reported that positively charged CDs (zeta potential of 27.6 mV) exhibited antibacterial activity by disrupting the bacterial cytoplasmic membrane. However, neutral (0.94 mV) and negatively charged (−19.5 mV) CDs interacted with the bacteria, resulting in the generation of ROS, and this is considered a major factor in inhibiting bacterial growth, leading to bacterial apoptosis (programmed cell death). Recent reports [24,48,49] on the antibacterial activity of CDs, especially in the *E. coli* system, have demonstrated that ROS production by activating the oxygen in air or water led to toxicity. In the present study, both the pristine and surface-modified CDs are anionic in nature, and the observed toxicity against *E. coli* might also be due to ROS production, and our LDH assay dataset confirms this notion, since LDH leakage is mainly attributed to oxidative stress. Other than ROS generation, the physical disruption of the *E. coli* cell membrane is also reported when interacting with negatively charged CDs [50]. Generally, in cases of physical disruption as a means of toxicity, it is widely stated that the electrostatic interaction between positively charged CDs and the negatively charged cell membranes of both Gram-positive and Gram-negative bacteria is the key mechanism [6]. Nevertheless, it is also reported that interactions between anionic charged CDs with slightly negatively charged bacterial surfaces are still possible due to other van der Walls forces, consisting of weak London dispersion forces and stronger dipole–dipole forces [51,52]. Recently, Qiang et al. [24] also reported that negatively charged carbon quantum dots have caused toxicity in *E. coli* and explained that adhesion of these CDs to the bacterial cell wall has led to ROS production, destruction of the cell membrane and causing cytoplasm leakage. Overall, our study also indicated that CDs with an overall anionic charge could also cause toxicity to bacterial cells. Furthermore, this work also demonstrated that the surface modification of CDs (urea-doped carbon

dots $_{(1:1)}$) by doping nitrogenous materials has also exhibited a maximum toxicity in *E. coli*. Earlier studies [48–50,53,54] have also shown that nitrogen-doped CDs had improved antibacterial activity, and this is attributed to amine functional groups on the surface of CDs having directly enhanced ROS production and or through its lower band gap, thus ultimately contributing to the bactericidal effect. These reports add strength to our findings that SMCDs (urea-doped CDs $_{(1:1)}$) exhibited the maximum toxicity. However, further and thorough explorations are needed and underway to document the underlying mechanisms of nitrogen-doped CDs in enhanced antibacterial activity.

3.8. Water Disinfection Potential of CDs

In order to assess the applicability of CDs as a disinfectant in water purification systems, two products, namely (i) CDs infused chitosan beads and (ii) pelletized CDs, were developed to immobilize CDs, and the efficiency of these two interventions were examined. The observations revealed that the CD-infused chitosan beads reduced the colonies of *E. coli* from 5.41×10^2 CFU/mL (control group) to 2.16×10^2 CFU/mL in comparison to pelletized CDs that decreased to 3.30×10^2 CFU/mL (Table 5). Thus, the CD-infused chitosan beads showed better water disinfection potential, as indicated by the reduction in the number of colonies (Figure 6). This can be explained with the findings of Kurt et al. [55], who developed chitosan fibers embedded with CDs from citric acid and assessed their antibacterial activity by using the disc diffusion method against *E. coli* and found that the inhibition of the zone increased from 1.8 ± 0.2 cm to 2.9 ± 0.4 cm against *E. coli* when increasing the concentration of the CDs from 2.9 mg to 5 mg.

Table 5. Water disinfection potential of CDs assessed with the developed prototypes.

Treatment	Number of Colonies ($\times 10^2$ CFU/mL)		Efficiency (%)
	Before Filtration	After Filtration	
Pelletized CDs	5.41	3.30	40
CD-infused chitosan beads	5.41	2.16	61

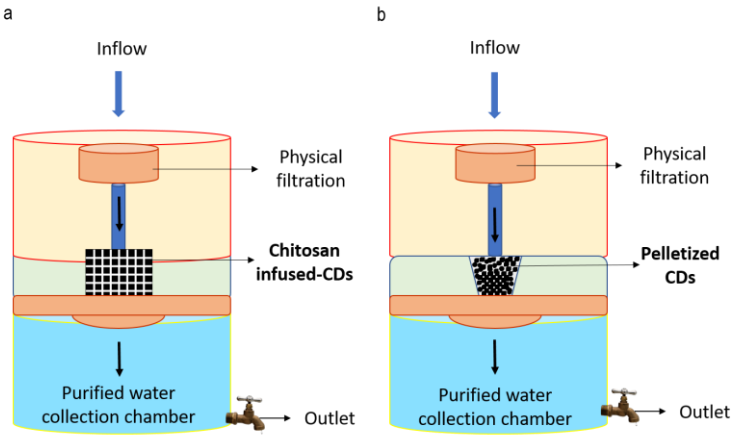

Figure 6. Lab-scale prototypesdesigned for assessing the water disinfection potential of CDs: (**a**) chitosan-infused CDs; (**b**) pelletized CDs.

3.9. Biosafety Studies of Synthesized CDs

Earthworms were used to investigate the biosafety of pristine CDs and urea-doped CDs $_{(1:1)}$, and the results revealed that the mortality rate was from 0 to 2000 ppm for a study period of 21 days (Figure 7). These observations are similar to the reports of Zhang et al. [56], who assessed the biosafety of carbon nanomaterials against earthworms by

using a filter paper contact test for 28 days and found that it was nontoxic even up to the concentration of 1000 mg/L. Several publications have also suggested that CDs are nontoxic to human cell lines. Liu et al. [57] reported that the CDs derived from wheat straw exhibited negligible cytotoxicity up to the concentration of 0.8 mg/mL, indicating that CDs are biocompatible in nature. In addition, Shi et al. [58] proved that amine-functionalized lignin CDs were nontoxic when tested against mouse macrophage cell lines at a dose of 100 µg/mL, for which the cell viability still remained 96.8%. Hence, the results of our biosafety studies with earthworms also suggested that CDs derived from coconut wastes, regardless of whether they are pristine or surface-modified, are biocompatible and safe.

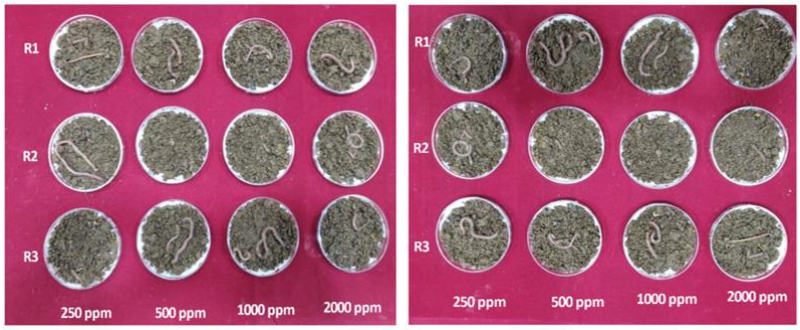

Figure 7. Biosafety test of pristine CDs (**left**) and urea-doped CDs $_{(1:1)}$ (**right**) on *Eisenia fetida*.

4. Conclusions

This study demonstrated that the novel sequential synthesis processes (pyrolysis and sonication method) is the best method to transform coconut wastes into CDs in the scope of large-scale production. Pristine CDs were anionic in nature, and the LDH assay confirmed their antibacterial ability against *E. coli*. The surface modification of CDs by doping urea during the synthesis process contributed to enhanced antibacterial properties. The principal mechanism behind the bactericidal effect of the CDs was the oxidative stress that was triggered as a result of the excessive production of ROS, and our measurement of the LDH leakage confirmed this mode of action. In addition, the amine functional groups on the surfaces of the CDs could have directly enhanced ROS production through its lower band gap, thus ultimately contributing to an enhanced bactericidal effect. Since these carbon nanomaterials are less than 10 nm in size, a challenge exists for employing them as a water disinfectant in purification systems. Thus, a suitable immobilization platform was identified by infusing CDs with a polymer, chitosan. A CD-based lab-scale prototype developed by utilizing urea-doped CDs infused with chitosan beads showed promising results for their applicability in water disinfection. Overall, this investigation highlighted that CDs are potential water disinfection agents that can be easily synthesized from waste biomasses so as to ensure sustainable solutions. Furthermore, this scientific endeavor has also opened up research avenues to redesign the prototypes for upscaling this nanotechnology to provide safe drinking water for all mankind.

Author Contributions: Conceptualization, S.K.R.; methodology, P.S.M. and S.K.R.; software, V.S.R.K.K. and M.P.; experimental study and validation, V.S.R.K.K. and K.P.D.; interpretation of the results, S.K.R., P.S.M. and M.M.; data curation and writing-original draft preparation, S.K.R., V.S.R.K.K. and K.P.D.; review and editing, K.S.S. and R.S. (Rajkishore Sunitha); visualization, K.P.D. and R.S. (Ruben Sakrabani); supervision, S.K.R. and P.S.M.; project administration, K.S.S., M.P., M.M. and N.S. and funding acquisition, S.K.R. All authors have read and agreed to the published version of the manuscript.

Funding: This research was funded by the Coconut Development Board, Kochi, Government of India (F.No.1272/2019/19029 dt.30.07.2019).

Institutional Review Board Statement: Not applicable.

Informed Consent Statement: Not applicable.

Data Availability Statement: Not applicable.

Acknowledgments: We express our gratitude to the Coconut Development Board (CDB), Kochi, Government of India, for funding this research program. The authors acknowledge the Department of Environmental Sciences and Centre for Agricultural Nanotechnology, Tamil Nadu Agricultural University, Coimbatore, India, for extending all the facilities.

Conflicts of Interest: The authors declare no conflict of interest.

References

1. Zheng, X.; Chen, G.; Li, Z.; Deng, S.; Xu, N. Quantum-mechanical investigation of field-emission mechanism of a micrometer-long single-walled carbon nanotube. *Phys. Rev. Lett.* **2004**, *92*, 106803. [CrossRef]
2. Mishra, V.; Patil, A.; Thakur, S.; Kesharwani, P. Carbon dots: Emerging theranostic nanoarchitectures. *Drug Discov. Today* **2018**, *23*, 1219–1232. [CrossRef]
3. Wang, L.; Li, W.; Yin, L.; Liu, Y.; Guo, H.; Lai, J.; Han, Y.; Li, G.; Li, M.; Zhang, J. Full-color fluorescent carbon quantum dots. *Sci. Adv.* **2020**, *6*, eabb6772. [CrossRef]
4. Shen, C.L.; Zang, J.H.; Lou, Q.; Su, L.X.; Li, Z.; Liu, Z.Y.; Dong, L.; Shan, C.X. In-situ embedding of carbon dots in a trisodium citrate crystal matrix for tunable solid-state fluorescence. *Carbon* **2018**, *136*, 359–368. [CrossRef]
5. Odonkor, S.T.; Mahami, T. *Escherichia coli* as a tool for disease risk assessment of drinking water sources. *Int. J. Microbiol.* **2020**, *2020*, 2534130. [CrossRef]
6. Dong, X.; Liang, W.; Meziani, M.J.; Sun, Y.P.; Yang, L. Carbon dots as potent antimicrobial agents. *Theranostics* **2020**, *10*, 671–686. [CrossRef]
7. Ghirardello, M.; Ramos-Soriano, J.; Galan, M.C. Carbon dots as an emergent class of antimicrobial agents. *Nano Mater.* **2021**, *11*, 1877. [CrossRef]
8. Chauhan, P.; Dogra, S.; Chaudhary, S.; Kumar, R. Usage of coconut coir for sustainable production of high-valued carbon dots with discriminatory sensing aptitude toward metal ions. *Mater. Today Chem.* **2020**, *16*, 100247. [CrossRef]
9. Chunduri, L.; Kurdekar, A.; Patnaik, S.; Dev, B.V.; Rattan, T.M.; Kamisetti, V.J. Carbon quantum dots from coconut husk: Evaluation for antioxidant and cytotoxic activity. *Mater. Focus* **2016**, *5*, 55–61. [CrossRef]
10. Abinaya, K.; Rajkishore, S.K.; Lakshmanan, A.; Anandham, R.; Dhananchezhiyan, P.; Praghadeesh, M. Synthesis and characterization of carbon dots from coconut shell by optimizing the hydrothermal carbonization process. *J. Appl. Nat. Sci.* **2021**, *13*, 1151–1157. [CrossRef]
11. Rani, U.A.; Ng, L.Y.; Ng, C.Y.; Mahmoudi, E. A review of carbon quantum dots and their applications in wastewater treatment. *Adv. Colloid Interface Sci.* **2020**, *278*, 102124. [CrossRef]
12. Tran, N.A.; Hien, N.Y.; Hoang, N.M.; Dang, H.T.; Huy, D.Q.; Quy, T.V.; Hanh, N.T.; Vu, N.H.; Dao, V.D. Carbon dots in environmental treatment and protection applications. *Desalination* **2023**, *548*, 116285. [CrossRef]
13. Lin, F.; Wang, Z.; Wu, F.-G. Carbon Dots for Killing Microorganisms: An Update since 2019. *Pharmaceuticals* **2022**, *15*, 1236. [CrossRef] [PubMed]
14. Zhu, W.; Mi, J.; Fu, Y.; Cui, D.; Lü, C. Multiple-cores@shell clustered carbon dots/P25/rGO nanocomposite as robust visible-light photocatalyst for organic pollutant degradation and water disinfection. *Appl. Surf. Sci.* **2021**, *538*, 148087. [CrossRef]
15. Elkodous, M.A.; Gharieb, S.; El-Sayyad; Youssry, S.M.; Hanady, G.N.; Gobara, M.; Elsayed, M.A.; El-Khawaga, A.M.; Kawamura, G.; Tan, W.K.; et al. Carbon-dot-loaded $Co_xNi_{1-x}Fe_2O_4$; x = 0.9/SiO_2/TiO_2 nanocomposite with enhanced photocatalytic and antimicrobial potential: An engineered nanocomposite for wastewater treatment. *Sci. Rep.* **2020**, *10*, 11534. [CrossRef]
16. Yang, X.; Sun, J.; Sheng, L.; Wang, Z.; Ye, Y.; Zheng, J.; Fan, M.; Zhang, Y.; Sun, X. Carbon dots cooperatively modulating photocatalytic performance and surface charge of O-doped g-C_3N_4 for efficient water disinfection. *J. Colloid Interface Sci.* **2023**, *631*, 25–34. [CrossRef] [PubMed]
17. Feng, R.Q.; Yuan, Z.Y.; Ren, T.Z. A facile hydrothermal method for preparation of fluorescent carbon dots on application of Fe^{3+} and fingerprint detection. *Methods Appl. Fluoresc.* **2019**, *7*, 035001. [CrossRef]
18. Perumal, S.; Atchudan, R.; Edison, T.; Lee, Y.R. Sustainable synthesis of multifunctional carbon dots using biomass and their applications: A mini-review. *J. Environ. Chem. Eng.* **2021**, *9*, 105802. [CrossRef]
19. Wang, Y.; Zhang, P.; Ye, C.; Fu, W.; Yuan, H.; Hu, P.; Liu, Y. Hexamethylenetetramine: An effective and universal nitrogen-doping reagent to enhance the photoluminescence of carbon nanodots. *New J. Chem.* **2018**, *42*, 3519–3525. [CrossRef]
20. Ma, Y.; Zhang, M.; Wang, H.; Wang, B.; Huang, H.; Liu, Y.; Kang, Z. N-doped carbon dots derived from leaves with low toxicity via damaging cytomembrane for broad-spectrum antibacterial activity. *Mater. Today Commun.* **2020**, *24*, 101222. [CrossRef]
21. Zhuang, P.; Li, K.; Li, D.; Qiao, H.; Wang, M.; Sun, J.; Mei, X.; Li, D. Correction: Assembly of Carbon Dots into Frameworks with Enhanced Stability and Antibacterial Activity. *Nanoscale Res. Lett.* **2021**, *16*, 125. [CrossRef] [PubMed]
22. Dager, A.; Uchida, T.; Maekawa, T.; Tachibana, M. Synthesis and characterization of mono-disperse carbon quantum dots from fennel seeds: Photoluminescence analysis using machine learning. *Sci. Rep.* **2019**, *9*, 14004. [CrossRef] [PubMed]
23. Kumar, V.B.; Porat, Z.; Gedanken, A. Facile one-step sonochemical synthesis of ultrafine and stable fluorescent C-dots. *Ultrason. Sonochem.* **2016**, *28*, 367–375. [CrossRef] [PubMed]

24. Qiang, S.; Zhang, L.; Li, Z.; Liang, J.; Li, P.; Song, J.; Guo, K.; Wang, Z.; Fan, Q. New Insights into the Cellular Toxicity of Carbon Quantum Dots to *Escherichia coli*. *Antioxidants* **2022**, *11*, 2475. [CrossRef] [PubMed]
25. Yan, X.; Rahman, S.; Rostami, M.; Tabasi, Z.A.; Khan, F.; Alodhayb, A.; Zhang, Y. Carbon quantum dot-incorporated chitosan hydrogel for selective sensing of Hg^{2+} ions: Synthesis, characterization, and density functional theory calculation. *ACS Omega* **2021**, *6*, 23504–23514. [CrossRef] [PubMed]
26. Keiller, B.G.; van Eyk, P.J.; Lane, D.J.; Muhlack, R.; Burton, A.B. Hydrothermal carbonization of Australian saltbush. *Energy Fuels* **2018**, *33*, 1157–1166. [CrossRef]
27. Sawalha, S.; Assali, M.; Nasasrah, A.; Salman, M.; Nasasrah, M.; Jitan, M.; Hilal, H.S.; Zyuod, A.J. Optical properties and photoactivity of carbon nanodots synthesized from olive solid wastes at different carbonization temperatures. *RSC Adv.* **2022**, *12*, 4490–4500. [CrossRef]
28. Ma, Z.; Ming, H.; Huang, H.; Liu, Y.; Kang, Z. One-step ultrasonic synthesis of fluorescent N-doped carbon dots from glucose and their visible-light sensitive photocatalytic ability. *New J. Chem.* **2012**, *36*, 861–864. [CrossRef]
29. Park, S.M.; Kim, T.G.; Chung, Y.D.; Cho, D.H.; Kim, J.; Kim, K.J.; Yi, Y.; Kim, J.W. Junction formation at the interface of CdS/CuInxGa (1− x) Se^2. *J. Phys. D Appl. Phys.* **2014**, *47*, 345302. [CrossRef]
30. Baweja, H.; Jeet, K. Economical and green synthesis of graphene and carbon quantum dots from agricultural waste. *Mater. Res. Express* **2019**, *6*, 0850–0858. [CrossRef]
31. Chaudhary, S.; Kumar, S.; Kaur, B.; Mehta, S.J. Potential prospects for carbon dots as a fluorescence sensing probe for metal ions. *RSC Adv.* **2016**, *6*, 90526–90536. [CrossRef]
32. Fatahi, Z.; Esfandiari, N.; Ehtesabi, H.; Bagheri, Z.; Tavana, H.; Ranjbar, Z.; Latifi, H.J. Physicochemical and cytotoxicity analysis of green synthesis carbon dots for cell imaging. *Excli J.* **2019**, *18*, 454–466.
33. Arvapalli, D.M.; Sheardy, A.T.; Alapati, K.C.; Wei, J. High Quantum Yield Fluorescent Carbon Nanodots for detection of Fe (III) Ions and Electrochemical Study of Quenching Mechanism. *Talanta* **2020**, *209*, 120538. [CrossRef]
34. Das, T.; Saikia, B.K.; Dekaboruah, H.; Bordoloi, M.; Neog, D.; Bora, J.J.; Lahkar, J.; Narzary, B.; Roy, S.; Ramaiah, D. Blue-fluorescent and biocompatible carbon dots derived from abundant low-quality coals. *J. Photochem. Photobiol. B* **2019**, *195*, 1–11. [CrossRef]
35. Manoharan, P.; Dhanabalan, S.C.; Alagan, M.; Muthuvijayan, S.; Ponraj, J.S.; Somasundaram, C.K. Facile synthesis and characterisation of green luminescent carbon nanodots prepared from tender coconut water using the acid-assisted ultrasonic route. *Micro Nano Lett.* **2020**, *15*, 920–924. [CrossRef]
36. Chauhan, P.; Mundekkad, D.; Mukherjee, A.; Chaudhary, S.; Umar, A.; Baskoutas, S. Coconut carbon dots: Progressive large-scale synthesis, detailed biological activities and smart sensing aptitudes towards tyrosine. *Nanomaterials* **2022**, *12*, 162. [CrossRef]
37. Gao, S.; Wang, X.; Xu, N.; Lian, H.; Xu, L.; Zhang, W.; Xu, C. From coconut petiole residues to fluorescent carbon dots via a green hydrothermal method for Fe^{3+} detection. *Cellulose* **2021**, *28*, 1647–1661. [CrossRef]
38. Arvapalli, D.M.; Sheardy, A.T.; Allado, K.; Chevva, H.; Yin, Z.; Wei, J. Design of curcumin loaded carbon nanodots delivery system: Enhanced bioavailability, release kinetics, and anticancer activity. *ACS Appl. Biol. Mater.* **2020**, *3*, 8776–8785. [CrossRef] [PubMed]
39. Zhang, Q.; Zhang, C.; Li, Z.; Ge, J.; Li, C.; Dong, C.; Shuang, S.J. Nitrogen-doped carbon dots as fluorescent probe for detection of curcumin based on the inner filter effect. *RSC Adv.* **2015**, *5*, 95054–95060. [CrossRef]
40. Mathew, S.A.; Praveena, P.; Dhanavel, S.; Manikandan, R.; Senthilkumar, S.; Stephen, A. Luminescent chitosan/carbon dots as an effective nano-drug carrier for neurodegenerative diseases. *RSC Adv.* **2020**, *10*, 24386–24396. [CrossRef]
41. Zheng, J.; Xie, Y.; Wei, Y.; Yang, Y.; Liu, X.; Chen, Y.; Xu, B. An efficient synthesis and photoelectric properties of green carbon quantum dots with high fluorescent quantum yield. *Nanomaterials* **2020**, *10*, 82. [CrossRef] [PubMed]
42. Kumar, R.; Kumar, V.B.; Gedanken, A. Sonochemical synthesis of carbon dots, mechanism, effect of parameters, and catalytic, energy, biomedical and tissue engineering applications. *Ultrason. Sonochem.* **2020**, *64*, 105009. [CrossRef] [PubMed]
43. Tomar, R.; Abdala, A.A.; Chaudhary, R.; Singh, N. Photocatalytic degradation of dyes by nanomaterials. *Mater. Today* **2020**, *29*, 967–973. [CrossRef]
44. Devkota, A.; Pandey, A.; Yadegari, Z.; Dumenyo, K.; Taheri, A. Glucosamine/β-alanine carbon dots use as DNA carriers into *E. coli* cells. *Front. Nanotechnol.* **2021**, *3*, 777810. [CrossRef]
45. Guo, B.; Liu, G.; Hu, C.; Lei, B.; Liu, Y. The structural characteristics and mechanisms of antimicrobial carbon dots: A mini review. *Mater. Adv.* **2022**, *3*, 7726–7741. [CrossRef]
46. Rajkishore, S.K.; Subramanian, K.S.; Natarajan, N.; Gunasekaran, K. Nanotoxicity at various trophic levels: A review. *Bioscan* **2013**, *8*, 975–982.
47. Bing, W.; Sun, H.; Yan, Z.; Ren, J.; Qu, X. Programmed bacteria death induced by carbon dots with different surface charge. *Communication* **2016**, *12*, 4713–4718. [CrossRef]
48. Kuo, W.S.; Chen, H.H.; Chen, S.Y.; Chang, C.Y.; Chen, P.C.; Hou, Y.I.; Shao, Y.T.; Kao, H.F.; Hsu, C.L.L.; Chen, Y.C.; et al. Graphene quantum dots with nitrogen-doped content dependence for highly efficient dual modality photodynamic antimicrobial therapy and bioimaging. *Biomaterials* **2017**, *120*, 185–194. [CrossRef]
49. Travlou, N.A.; Giannakoudakis, D.A.; Algarra, M.; Labella, A.M.; Rodriguez-Castellon, E.; Bandosz, T.J. S-and N-doped carbon quantum dots: Surface chemistry dependent antibacterial activity. *Carbon* **2018**, *135*, 104–111. [CrossRef]

50. Das, P.; Ganguly, S.; Bose, M.; Mondal, S.; Choudhary, S.; Gangopadhyay, S.; Das, N.C. Zinc and nitrogen ornamented bluish white luminescent carbon dots for engrossing bacteriostatic activity and Fenton based bio-sensor. *Mater. Sci. Eng.-C* **2018**, *88*, 115–129. [CrossRef] [PubMed]
51. Maruthapandi, M.; Saravanan, A.; Luong, J.H.T.; Gedanken, A. Antimicrobial properties of polyaniline and polypyrrole decorated with zinc-doped copper oxide microparticles. *Polymers* **2020**, *12*, 1286. [CrossRef] [PubMed]
52. Saravanan, A.; Maruthapandi, M.; Das, P.; Luong, J.H.T.; Gedanken, A. Green Synthesis of Multifunctional Carbon Dots with Antibacterial Activities. *Nanomaterials* **2021**, *11*, 369. [CrossRef] [PubMed]
53. Kang, J.; Kang, D. Effect of amino acid-derived nitrogen and/or sulfur doping on the visible-light-driven antimicrobial activity of carbon quantum dots: A comparative study. *Chem. Eng. J.* **2021**, *420*, 129990. [CrossRef]
54. Kung, J.C.; Tseng, I.T.; Chien, C.S.; Lin, S.H.; Wang, C.C.; Shih, C. Microwave assisted synthesis of negative charge carbon dots with potential antibacterial activity against multi-drug resistant bacteria. *RSC Adv.* **2020**, *10*, 41202–41208. [CrossRef] [PubMed]
55. Kurt, S.B.; Sahiner, N. Chitosan based fibers embedding carbon dots with anti-bacterial and fluorescent properties. *Polym. Compos.* **2021**, *42*, 872–880. [CrossRef]
56. Zhang, L.; Hu, C.; Wang, W.; Ji, F.; Cui, Y.; Li, M. Acute toxicity of multi-walled carbon nanotubes, sodium pentachlorophenate, and their complex on earthworm *Eisenia fetida*. *Ecotoxicol. Environ. Saf.* **2014**, *103*, 29–35. [CrossRef]
57. Liu, S.; Liu, Z.; Li, Q.; Xia, H.; Yang, W.; Wang, R.; Li, Y.; Zhao, H.; Tian, B. Facile synthesis of carbon dots from wheat straw for colorimetric and fluorescent detection of fluoride and cellular imaging. *Spectrochim. Acta Part A* **2021**, *246*, 118964. [CrossRef]
58. Shi, Y.; Liu, X.; Wang, M.; Huang, J.; Jiang, X.; Pang, J.; Xu, F.; Zhang, X. Synthesis of N-doped carbon quantum dots from bio-waste lignin for selective irons detection and cellular imaging. *Int. J. Biol. Macromol.* **2019**, *128*, 537–545. [CrossRef]

Novel synthesis of carbon dots from coconut wastes and its potential as water disinfectant

Rajkishore, Subramani Krishnaraj

2023-07-02

Rajkishore SK, Devadharshini KP, Sathya Moorthy P, et al., (2023) Novel synthesis of carbon dots from coconut wastes and its potential as water disinfectant. Sustainability, Volume 15, Issue 14, July 2023, Article Number 10924

https://doi.org/10.3390/su151410924